ANALYSIS OF THE ANNUAL CYCLE OF THE PRECIPITABLE WATER VAPOR OVER SPAIN FROM 10-YEAR HOMOGENIZED SERIES OF GPS DATA

J. P. Ortiz de Galisteo[1, 2], Y. Bennouna[2], C. Toledano[2], V. Cachorro[2], P. Romero[3], M. I. Andrés[4], B. Torres[2]

[1] AEMET (Meteorological State Agency), Territorial Delegation of "Castilla y León", Spain.

[2] GOA-UVA (Group of Atmospheric Optics), University of Valladolid, Spain.

[3] CIAI (Izaña Atmospheric Research Center, AEMET), Spain.

[4] Junta de Castilla y León – Consejería de Educación, Spain.

Corresponding Author:

J.P. Ortiz de Galisteo

e-mail: jportiz@goa.uva.es

Keywords: precipitable water vapor; PWV; annual cycle; GPS; climatology.

Abstract

This study reports a characterization of the precipitable water vapor (PWV) at ten sites over Spain from 10 years of hourly data from ground-based GPS receivers. The GPS-PWV data series turned out to be inhomogeneous due to the change in the calibration procedure of the variations of the antenna phase center in November 2006. Radiosonde data were used to homogenize the GPS data series and to assess the quality of the GPS measurements. The annual average value of PWV ranges from 14.5 to 20.0 mm, with an average of 18.3 ± 1.9 for the entire Spain. The highest values are registered at the sites on the coast, especially on the Mediterranean coast, and the lowest ones at inland sites. The PWV presents a clear annual cycle, with a minimum in winter and maximum at the end of the summer. However, the southwestern sites present a relative minimum in July. This minimum seems to be related with the presence of drier air masses in the atmospheric layers between 1 and 4 km altitude. The amplitude of the cycle ranged from 8.9 to 18.7 mm. The largest amplitudes are found at the Mediterranean coastal sites (approx. 15-19 mm) and the lowest ones at inland sites (approx. 9-10 mm). A harmonic analysis of the annual cycle showed that the 12-month period harmonic explains, on average, over 96 % of the variance. The average annual regime of PWV followed the cycle of the temperature, except for the relative minimum of PWV in July at the southwestern sites.

1. Introduction

Precipitable water vapor (PWV) is defined as the height of liquid water that would be obtained if the total amount of water vapor in an atmospheric column of unit area were condensed into a layer on that surface. PWV plays a crucial role in many atmospheric processes, such as the meridian transference of energy, the greenhouse effect, the radiative balance, the structure and evolution of storm systems, etc. Nevertheless, and despite its importance, its knowledge is limited due to the lack of high spatial-temporal resolution observations. Precisely one of the problems of measuring PWV is its high temporal and spatial variability that takes place at scales much smaller than other meteorological variables.

A large number of instruments have been developed to measure PWV, each one with its strong points and drawbacks. Radiosondes provide the longest data series. However, the high cost of each launch explains the low spatial and temporal resolution of radiosonde.

PWV can also be obtained from the measurements of the ground-based GPS receivers (Bevis et al., 1992). These equipments can provide data with high temporal resolution (one-hour or less) in all weather conditions, and during both day and night time. The proliferation in recent years of networks of high precision GPS receivers permits a more complete study of this atmospheric component. Thus, GPS system appears at this moment as one of the most powerful technique to study PWV (Hagemann et al., 2003; De Haan S. de, 2006; Wang et al., 2007; Heise et al., 2009). It has already been used in recent studies to analyze its annual cycle (Jin and Luo, 2009), the diurnal cycle (Ortiz de Galisteo et al., 2011), the long-term trends (Nilsson and Elgered, 2008), the monitoring of meteorological episodes (Champollion et al., 2004; Seco et al., 2009) or the improvement in precipitation forecasting (Marcus et al., 2007).

The determination of PWV from ground-based GPS receivers is based on the delay produced by the atmosphere on the arrival of the signal to the Earth's surface. This delay can be divided in ionospheric and tropospheric components. The ionospheric delay is dispersive. So that, in order to quantify and remove the effect of the ionosphere in the propagation of the signal (Brunner and Gu, 1991) the GPS satellites transmit at two carrier frequencies. On the contrary, the tropospheric delay is non-dispersive. The delay in the troposphere is determined by the refractive index along the signal path. The refractivity of the atmosphere is a function of temperature, pressure, and water vapor content. Water vapor is the only gas in the troposphere that has a permanent dipole moment that contributes to the dipolar component of the atmospheric refractivity. Thus, the zenith tropospheric delay (ZTD) can be divided into a hydrostatic delay (ZHD), associated with the dipole moment induced, and into a wet delay (ZWD), associated with the permanent dipole moment of water vapor (Saastamoinen, 1972). The ZTD can be calculated from the own measurements of GPS receivers by complex inversion algorithms (Tralli et al., 1990; Herring et al., 1990; Duan et al., 1996). The ZHD can be modeled if the pressure at the surface is known. The ZWD is obtained subtracting the ZHD from the ZTD. Subsequently, the ZWD can be transformed into PWV from the water-vapor-weighted mean temperature (Davis et al., 1985). Approximately 1 mm of PWV produces a 6.35 mm delay, but this factor can oscillate about 20 %, depending on the location, the altitude, the season, and the meteorological conditions (Bevis et al., 1994).

The quality of the PWV data from GPS receivers has been proved by comparisons with different instruments and techniques by several authors (Ohtani and Naito, 2000; Bokoye et al., 2003; Wang et al., 2007; Heise et al., 2009; Schneider et al., 2009). The root mean square (*RMS*) are usually between 1 and 3 mm. Nevertheless, on November 6, 2006, the International GNSS Service (IGS) adopted an absolute calibration model for the phase center variations (PCV) of the antennas of the GPS satellites and receivers, instead of the relative model used until that date. This change led to an improvement in the accuracy of the determination of the station position, and consequently in the post-processed products, such as the ZTD and the PWV (Steigenberger et al., 2007; Thomas et al., 2011). Prior to that date, the GPS data presented a wet bias of 2-3 mm in the PWV when compared with radiosonde data, whereas after that date this bias has been practically reduced to zero (Ortiz de Galisteo et al., 2010).

There are studies in the literature concerning the climatology of the PWV based on: radiosonde data (Reitan, 1960), satellite observations (Gao et al., 2004), reanalysis of numerical weather prediction (NWP) models (Zveryaev et al., 2008), and more recently on

GPS data (Jin and Luo, 2009). Most of them are global (Tuller, 1968; Gaffen et al., 1992; Randel et al., 1996), but, as aforementioned, they do not describe efficiently the high spatial variability of PWV. Although there are other studies on regional scale (Jin et al., 2008; Morland et al., 2009), none of them is focused on the whole Spanish territory but rather on some specific area (Torres et al., 2010). Spain is located between two seas with different characteristics, the Atlantic Ocean and the Mediterranean Sea. It also has an abrupt and complicated relief, with mountain ranges running from west to east and from north to south, two high plateaus and some large river valleys. Due to this geographical configuration and the fact that the water vapor content at low levels, where its amount is the highest, is very influenced by mesoscale factors, several areas with different PWV climatology can be expected; therefore, a good spatial resolution is needed. Therefore, in this study GPS data are used with the aim to characterize the annual regime of PWV over Spain. The GPS receivers constitute the densest ground network available. Only satellite data can offer better spatial coverage, but with worse temporal resolution and worse accuracy.

2. Methodology and data sets

Hourly data from the GPS receivers over Spain belonging to the European Reference Frame (EUREF) were used in the present study. The number of GPS sites has increased considerably in recent years, but in order to characterize the annual regime of the PWV with a certain reliability, a compromise had to be reached between the number of available stations to achieve a better spatial coverage, and the length of the data series. Hence, only those stations with data back to 2002 were selected. These sites are shown on a map of the Iberian Peninsula in Fig. 1, and their geographical coordinates are shown in Table 1. To avoid any kind of bias, only complete years of data were considered, from January 2002 to December 2011.

The ZTD data were obtained from the EUREF Permanent Network website (http://epncb.oma.be/). Within the routine analysis of a network of ground-based GPS receivers, the tropospheric parameters are a by-product. Among all EUREF Analysis Centers, the data generated by the National Geographic Institute of Spain (IGNE) were selected. The IGNE processes the ZTD of all the EUREF stations over Spain using the Bernese V5.0 software and the final precise orbits of the satellites provided by the IGS (Kruse et al., 1999), in order to achieve the highest accuracy. The ZTD was transformed into PWV using pressure and temperature data registered in the nearest meteorological station of the Meteorological State Agency (AEMET), according to the procedure described by Bevis et al. (1992). The meteorological data were corrected by the difference of altitude between the GPS receiver and the meteorological station. To do so, a standard atmosphere with a vertical gradient of temperature of 6.5 ºC/km was considered. In addition, the meteorological data were interpolated to the time of the ZTD measurements. The temperature data were linearly interpolated, whereas the pressure data were interpolated taking into account the barometric tide, which over Spain presents a semidiurnal cycle with the maximum values around 1000 and 2200 UTC, the minimum around 0400 and 1600 UTC, and a mean amplitude of 0.5 hPa (Ray and Ponte, 2003). It was done this way because the calculation of the PWV is more sensitive to the uncertainties in pressure data than in temperature data. An error of 1 hPa produces approximately an error of 0.36 mm on PWV (Hagemann et al., 2003).

The water-vapor-weighted mean temperature of the atmosphere T_m (Davis et al., 1985), which is necessary to transform the ZWD into PWV, was calculated from the surface temperature T_s using the equation $T_m = 61.9 + 0.75\ T_s$. This equation has been derived empirically in this study on the basis of 37,179 sounding profiles spanning a 9-year interval from all the radiosonde stations over Spain, instead of the similar equation obtained by Bevis et al. (1992) with sounding data from the USA. This linear regression has a bias of 0.1 mm and a *RMS* of 3.2 K. Different expressions were tried for each season of the year, for daytime and nighttime, and for each radiosonde station. However, the correlation between both magnitudes (T_m and T_s) did not improve. This T_m-T_s relationship does not take into account the fact that T_s has an amplitude of the diurnal cycle much higher than T_m (Wang et al., 2005). To remove it, the T_s was damped according to the expression $T_{sd} = 0.25\ T_s + 0.75\ T_{sm}$, where T_{sm} is the daily mean of the surface air temperature (Morland et al., 2009).

The PWV data from each GPS site were analyzed as follows. First, the daily means were calculated as the arithmetic mean of all the available hourly data for each day. If the number of available data in one day was lower than twelve, the whole day was rejected. Nevertheless, less than 1 % of the days presented missing data. This average is very representative because the hourly frequency takes into account the complete temporal evolution of the PWV along the day. Afterward, the daily data of each month were averaged to obtain the monthly means. At this point, the months with more than half of the days without data were discarded. With this criterion, the series of the monthly means presented only a few gaps, which were filled according to the following procedure. The monthly anomalies were obtained subtracting the annual average cycle from the series of the monthly means. Subsequently, the anomalies were interpolated linearly to fill any gap. And finally, the annual average cycle was added again.

Like any other data series, GPS measurements are affected by changes in the instrumentation or in the calculation procedures. In these cases, the series must undergo homogenization (Aguilar et al., 2003), a statistical process that tries to remove the unwanted perturbations and let the climatological series reveal climate variations only. Because of the change in the calibration model of the PCV for GPS antennas on November 6, 2006, the data series will exhibit an inhomogeneity, which must be removed before any further analyses. To know what kind of homogenization test could be used, firstly the monthly series were subjected to the Lilliefors test for normality (Lilliefors, 1967). In all cases the computed p-value was lower than the significance level (5 %), meaning that the series did not follow a normal distribution, so that, a non-parametric test had to be applied. Thus, the monthly series underwent the Pettitt´s test (Pettitt, 1979). This test revealed a split in November 2006 in all the series. Although the test was only significant at confidence level 5 % for *acor* and *cace* sites, we knew by the metadata that a change took place in November 2006. Besides, when a Wilcoxon-Mann-Whithey sign test (Lanzante, 1996) was applied to make a comparison between the series before and after Nov 2006, we obtained that both samples did not follow the same distribution.

The R-package CLIMATOL 2.0 (Guijarro 2011) was used in order to homogenize the series. This software package uses the Standard Normal Homogeneity Test (SNHT) (Alexandersson, 1986) to detect shifts in the mean of the series and a relative homogenization method, where the problem time series is compared to one or more reference series that should be in the same climatic region. If the reference series is well chosen, it should show the same climatic variations as the problem series, and any differences will be due to artificial factors. In the R-package CLIMATOL 2.0, the homogeneity tests are applied on a difference series between the problem station and a reference series, constructed as a weighted average of series from nearby stations on a proximity criteria only. Since the presence of sharp geographical boundaries can lead to the use of nearby badly correlated stations to compute the reference series, our area of interest was divided in four sub-areas: Cantabrian coastal, Mediterranean coastal, Atlantic coastal, and inland, and the homogeneity process was independently applied to each area. If this division is not done the whole region is not climatically homogeneous and some erroneous inhomogenities that do not match with the metadata appear. At this point, data from radiosonde stations (Fig. 1) were used as reference. The radiosonde data were downloaded from the University of Wyoming website (http://weather.uwyo.edu/upperair/sounding.html). The R-package CLIMATOL 2.0 uses a type II regression (Sokal and Rohlf, 1969) to recalculate the series after a shift has been detected.

Subsequently, the homogenized series were averaged over each month of the year to obtain a long-term annual cycle. The amplitude was computed as the difference between the maximum and minimum values of the cycle. The ratio between these two values was also calculated to characterize the annual cycle. In addition, the annual cycle of the temperature was computed for the same period (2002-2011) at the meteorological stations, in order to analyze the relationship between both variables (PWV and temperature). Finally, to validate the characteristic of the annual cycle of PWV obtained in this study with the GPS data, the results from *acor*, and *vill* were contrasted with those obtained from 30-year climatology (1982-2011) at the nearby radiosonde stations (stations numbers: 08001 and 08221).

3. Results

This section contains some general results for the whole period based on the monthly means. Thereafter, the annual cycle of PWV is described. Finally the observed minimum of PWV in July is investigated.

3.1. General results

Table 2 shows statistics of the monthly means for each site. The average PWV ranges from 14.5 mm to 20.0 mm. The PWV and its variability (SD) are larger at the sites on the coast, especially on the Mediterranean coast, than at the inland sites. The stations on the Atlantic coast registered values only slightly lower than the stations on the Mediterranean coast. The positive asymmetric coefficient indicates that the mass of the distribution is more concentrated on the left of the frequency histogram, i.e. it has relatively fewer high values. The negative kurtosis means that there is a lower probability than in a normally distributed variable of values around the mean, and a higher probability of extreme values.

3.2. Annual cycle

The graph of the temporal evolution of the monthly means presents a clear annual cycle at all sites. This fact was confirmed by the spectral analysis of the monthly series, which was applied in order to study the number of terms in a Fourier expansion required to describe the PWV variation. The Lomb-Scargle periodogram (Hocke, 1998) only shows a significant peak for the 12-month period, indicating that it is sufficient to use an annual term to describe the seasonal variations of PWV. Figure 2 deplots the annual cycle obtained for each GPS site according to the abovementioned procedure. The PWV presents a minimum in winter and a maximum at the end of the summer. The winter minimum takes place in January or February, meanwhile, the maximum takes place in August (in September at *sfer*). The decrease in autumn is steeper than the increase during the spring. The autumn, and especially November, presents the highest dispersion of the monthly values. A weak relative minimum appears in July at the sites located in the southern quadrant of the Iberian Peninsula, not for all Julys though for most of them, and also in the average annual cycle. Although this minimum is not very deep, the maximum decrease compared to June is only 1.6 mm (*cace*), it might be a significant characteristic. The depth of this relative minimum decreases when the latitude increases. At sites located in the southeast (*alme*), the minimum does not appear, but the increase rate of PWV from June to July diminishes.

The largest amplitudes of the annual cycle were recorded at the Mediterranean coastal sites. This is mainly because the annual maximum values stand out in this area due to the high water temperature of the sea and to the sea breeze regime that transport a great amount of water vapor from the sea, which is particularly strong in summer in this area. Whereas in winter, the westerly dominant winds transport an air mass of oceanic origin that becomes drier when passing through the Iberian Peninsula before reaching the Mediterranean sea. This means the minimum values are slightly lower than at the Atlantic coastal sites. The weak amplitude of the inland sites is owed to the lack of moisture sources. They present low values of PWV in both summer and winter. The ratio between the maximum and minimum values of the annual regime ranges from 1.8 to 2.5.

Including all sites, for Spain the average annual value of the PWV (~18.3 mm) and the ratio of the maximum to minimum of the annual regime (~ 2.2) correspond with the middle and high latitude oceanic humidity regime of the Gaffen's classification (Gaffen et al., 1992). This regime is characterized by an annual cycle with a maximum at the end of the summer in phase with temperature, a ratio of the maximum to minimum from 1.5 to 3, and an annual mean value from 5 to 20 mm.

The annual cycle of the PWV was subjected to a harmonic analysis. The first four harmonics with period 12, 6, 4 and 3 months were considered. The first harmonic (12-month period) was dominant at all the sites, with a mean amplitude of approx. 7 mm (half of the peak-to-peak value) and a phase of 8 (month of the maximum). On average, the 12-month period harmonic explains over 96 % of the variance, whereas the other harmonics explain less than 1 %. It is only remarkable the variance explained by the 6-month period harmonic (5 %) at *sfer*, close to the Strait of Gibraltar. In that area the air flow usually blows either from the Atlantic Ocean or from the Mediterranean Sea, two zones with different temperature of the sea water, so that, the coming air masses contain different ammount of PWV. In winter the frequency of air masses from the Mediterranean sea is higher than the frequency of air masses from the Atlantic ocean, and conversely in summer.

The annual cycle of PWV follows approximately the temperature cycle (Fig. 3), except for the relative minimum of PWV in July at the southwestern sites, which does not match the temperature pattern. In general, the higher the temperature is the higher the PWV. This is true for each site individually. However, when different sites are compared, other factors such as the proximity to the coast, the altitude, the wind regime, etc. make the differences. For example, the maximum of temperature at inland and at Mediterranean coastal sites is quite similar, and higher than at the Atlantic coastal sites, whereas the maximum of PWV at inland sites is the lowest one. The amplitude of the annual cycle of the temperature and of the PWV does not keep the same ratio either, but it also depends on the latitude and the inland or coastal nature of the location. The annual temperature variation at inland sites is maximum whereas the corresponding variation of PWV is minimum, and the opposite applies to the coastal sites. Nevertheless, a linear regression of PWV vs temperature can be established. The correlation between the monthly series of both variables is higher for coastal sites than for inland sites (R^2 ranges from 0.71 to 0.93), except for *sfer* due to the minimum of PWV in July (R^2=0.68) (Table 3).

In order to evaluate whether the results presented here are representative on the long-term, the 10-year annual cycle obtained from radisonde data at the stations *08001* and *08221* (close to the GPS sites of *acor* and *vill*) was compared with that obtained from 30 years of data (1982-2011) (Fig. 4). The determination coefficient (R^2) between both cycles was 0.99. The mean difference was 0.2 mm (0.9 %) and 0.3 mm (1.5 %) respectively, being the PWV higher in 2002-2011 than in 1982-2011. The maximum difference always takes place always in June, 1.1 mm at *08001* and 1.0 at *08221* (5 %,). The abovementioned relative minimum in July is masked in the 1982-2011 series. It seems to indicate that this minimum is more likely to be associated with an increase of PWV in June in the later years, than with an actual decrease in July.

3.3. Analysis of the minimum of PWV in July

The analysis of the vertical distribution of the PWV from the radiosondes at Gibraltar can provide further insight on this subject. To do this, the vertical profiles of absolute humidity from radiosondes were averaged over each month of the year.

The vertical distribution of the absolute humidity relative to the values of July at Gibraltar (Fig. 5) shows an increase of humidity in the lowest layers of the atmosphere from June to August. This agrees with the increase in the surface temperature. However, above 1 km altitude the humidity is higher in June than in July. The highest difference is reached about 2 km altitude (0.7 g/m^3). The higher humidity above 1 km in June balances out, and even exceeds, the higher humidity in the lower layers in July. As a result, the total PWV in July decreases in comparison with June. The accumulated humidity from the surface tends to be higher in July than in June up to about 1 km, above this altitude level the trend reverses, and above 2.5 km it is higher in June than in July (Fig. 6). The difference stabilizes above 4 km, pointing out that the contribution of these layers in both cases is the same. This proves that although evaporation is higher in July than in June, the relative minimum of PWV is due to the fact that the air masses arriving at this area are drier in average in July than in June.

The monthly composites of the geopotential height at 850 hPa pressure level (approx. 1500 m) from the NCEP/NCAR reanalysis (Kalnay et al., 1996) show a trough in June over the area of interest (Fig. 7). Hence, the atmospheric flow has a higher meridian component. In July, the inter-tropical convergence zone (high pressures) moves toward higher latitudes, making the atmospheric circulation more zonal. This fact agrees with a backward-trajectory study at different altitude levels of El Arenosillo station (37.1º N – 6.7º W, on the south-west Atlantic coast, Huelva) for the period 2000-2005 carried out by Toledano et al. (2009). This study shows a decrease in the arrival frequency of African air masses above 1.5 km in July in relation to June, and an increase of air masses of Atlantic origin. Starting from this study, the air mass type arriving at El Arenosillo at 1.5 km altitude level was correlated with the PWV. It was obtained that the PWV is higher when the air mass is continental tropical (from African origin) than when it is maritime (from Atlantic origin) (Fig. 8).

Due to the presence of the Sahara desert, the continental tropical air masses contain a great amount of mineral dust. The intense heating of the desert surface during summer produces a low-pressure system of thermal origin over north Africa. The strong convection injects a great amount of Saharan dust to the middle and high levels of the atmosphere. At these levels, the dust is transported toward Spain. The intrusion of Saharan air masses is characterized by an increase in the aerosol optical depth (AOD), and a decrease in the Angstrom exponent (AE) that is related with the aerosol size (Cachorro et al., 2000; Toledano et al., 2007a). Typical values of Saharan air masses are: AOD (440 nm) higher than 0.25, and AE lower than 1 that indicates coarse particle predominance (Toledano et al., 2007b). The annual evolution of the AOD at the AERONET station of El Arenosillo also shows a relative minimum in July (Bennouna et al., 2011). The analysis of the PWV data in relation with the aerosol type of El Arenosillo from the period 2002-2009, reveals that the average PWV is higher when the aerosol type is desert dust than when is marine or continental (Table 4). This is also in agreement with the hypothesis that the relative minimum of PWV in July may be produced by fewer intrusions at low-to-middle levels (1 to 4 km) of Saharan air masses in July in comparison to June.

4. Conclusions

PWV plays a crucial role in many atmospheric processes. Nevertheless, its knowledge has been limited due to the lack of high spatial-temporal resolution observations. The proliferation in recent years of networks of high precision GPS receivers permits a more complete study of this atmospheric component. Thus, GPS system appears at this moment as one of the most powerful technique to study PWV. This study provides the first characterization of PWV over Spain. The behavior of PWV has been studied at ten locations from 10 years of data acquired by ground-based GPS receivers. The data series had to undergo a homogenization process to remove the unwanted perturbations, which led to a wet bias of 2-3 mm, due to a change in November 2006 in the calibration procedure of the PCV for GPS antennas. As expected, the annual cycle of PWV presents a maximum in summer and a minium in winter at all sites, with amplitudes that can vary significantly depending on the geographical location of the site. However, an unexpected feature corresponding to a relative minimum appears in July for the sites located in the southern quadrant of the Spain. On average, the annual regime of PWV over Spain corresponds with the middle and high latitude oceanic humidity regime of the Gaffen's classification. According to a harmonic analysis, the annual cycle can be mostly explained by the 12-month period harmonic. The corretalion between the annual cycle of PWV and temperature depended on factors such as the proximity to the coast, the altitude, the wind regime, etc.

From the comparison between the cycles obtained for ten years (2002-2011) and thirty years (1982-2011) of sounding data, it can be concluded that the characterization of the PWV over Spain presented in this study is fairly close to its climatological values. This allows to carry out a representative study on the long-term with only 10 years of data, and this makes possible to include data from more locations. Currently there are already 28 GPS stations belonging to EUREF over Spain. This denser GPS network will permit further deeper analysis of the local characteristics of the PWV.

Acknowledgements

Financial support was provided by the Spanish CICYT and the ESF under the projetcs CGL2009-09740, CGL2011-23413, CGL2012-33576, CGL2011-13085-E. We also thank to ITACYL for the finnatial support of the EVACYL project.

The authors are grateful to the members of the EUREF and IGN teams for providing GPS data, and the NOAA/ESRL Physical Science Division, Boulder Colorado for the images from their Web site at http://www.esrl.noaa.gov/psd/.

References

Aguilar, E., I. Auer, M. Brunet, T.C. Peterson, and J. Wieringa, 2003: Guidelines on climate metadata and homogenization. WCDMP-No. 53, WMO-TD No. 1186. World Meteorological Organization, Geneve.

Alexandersson, H., 1986: A homogeneity test applied to precipitation data, *J. Climatol*., 6:661–675.

Bennouna, Y.S., V.E. Cachorro, C. Toledano, A. Berjon, N. Prats, D. Fuertes; R. Gonzalez; R. Rodrigo, B. Torres, and A.M. de Frutos, 2011: Comparison of atmospheric aerosol climatologies over southwestern Spain derived from AERONET, MODIS and OMI. *Remote Sensing Environment*, 115, 1272–1284.

Bevis, M., S. Businger, T.A. Herring, C. Rocken, R.A. Anthes, and R.H. Ware, 1992: GPS Meteorology: Remote Sensing of Atmospheric Water Vapor using the Global Positioning System. *J. Geophys. Res.*, 97, 15787–15801.

Bevis, M., S. Businger, S. Chiswell, T.A. Herring, R.A. Anthes, C. Rocken, and R.H. Ware, 1994: GPS Meteorology: Mapping Zenith Wet Delays onto Precipitable Water, *J. Appl. Meteorol*, 33, 379–386.

Bokoye, A.I., A. Royer, N.T. O'Neill, P. Cliché, L.J.B. McArthur, P.M. Teillet, G. Fedosejevs, and J.M. Thériault, 2003: Multisensor analysis of integrated atmospheric water vapor over Canada and Alaska, *J. Geophys. Res.*, 108(D15), 4480, DOI: 10.1029/2002JD002721.

Brunner, F. K., and M. Gu, 1991: An improved model for the dual frequency ionospheric correction of GPS observations, *Manusc. Geod.*, 16, 205–214.

Cachorro, V.E., P. Duran, R. Vergaz, and A.M. De Frutos, 2000: Measurements of the atmospheric turbidity of the north-center continental area in Spain: spectral aerosol optical thickness and Angstrom turbidity parameters, *J. Aerosol Sci.*, 31, 687-702.

Champollion, C., F. Masson, J. Van Baelen, A. Walpersdorf, J. Chéry, and E. Doerflinger, 2004: GPS monitoring of the tropospheric water vapor distribution and variation during the 9 September 2002 torrential precipitation episode in the Cévennes (southern France), *J. Geophys. Res.*, 109, D24102, DOI:10.1029/2004JD004897.

Davis, J.L., T.A. Herring, I.I. Shapiro, A.E. Rogers, and G. Elgered, 1985: Geodesy by radio interferometry: Effects of atmospheric modelling errors on estimates of baseline length, *Radio Sci.*, 20, 1593–1607.

De Haan, S., 2006: National/regional operational procedures of GPS water vapor networks and agreed international procedures, WMO - World Meteorological Organization. Instruments and Observing Methods, Report No. 92.

Duan, J., M. Bevis, P. Fang, Y. Bock, S. Chiswell, S. Businger, C. Rocken, F. Solheim, T. van Hove, R. Ware, S. McClusky, T.A. Herring, and R.W. King, 1996: GPS Meteorology: Direct Estimation of the Absolute Value of Precipitable Water, *J. Appl. Meteorol.*, 35, 830–838.

Gaffen, D.J., A. Robock, and W.P. Elliot, 1992: Annual cycle of tropospheric water vapor, *J. Geophys. Res.*, 97, 18185–18193.

Gao, B.C., P. K. Chan, and R.R. Li, 2004: A global water vapor data set obtained by merging the SSMI and MODIS data, Geophys. Res. Let., 31, 18, p. L18 103. DOI: 10.1029/2004GL020656.

Guijarro, J.A., 2011: User's guide to climatol. An R contributed package for homogenization of climatological series, Report, State Meteorological Agency, Balearic Islands Office, Spain, available at: http://webs.ono.com/climatol/climatol.html.

Hagemann, S., L. Bengtsson, and G. Gendt, 2003: On the determination of atmospheric water vapor from GPS measurements, *J. Geophys. Res.*, 108, 4678, DOI:10.1029/2002JD003235, D21.

Heise, S., M. Bender, G. Beyerle, G. Dick, G. Gendt, T. Schmidt, and J. Wickert, 2009: Integrated water vapor from IGS ground-based GPS observations: Initial results from a global 5-minute data set, *Annales Geophysicae*, 27, 7, 2851–2859.

Herring, T., J.L. Davis, and I.I. Shapiro, 1990: Geodesy by radio interferometry: The application of Kalman filtering to the analysis of very long baseline interferometry data, *J. Geophys. Res.*, 95, 12,561–12,581.

Hocke, K., 1998: Phase estimation with Lomb-Scargle periodogram method, *Ann. Geophys.*, 16, 356–358.

Jin, S., Z. Li, and J. Cho, 2008: Integrated Water Vapor Field and Multiscale Variations over China from GPS Measurements, *J. Appl. Meteorology Climatology*, 47, 3008–3015, DOI: 10.1175/2008JAMC1920.1.

Jin, S.G. and O.F. Luo, 2009: Variability and climatology of PWV from global 13-year GPS observations, *IEEE Trans. Geosci. Remote Sens.*, Vol. 47, NO. 7, July 2009, DOI: 10.1109/TGRS.2008.2010401.

Kalnay, E. and Coauthors, 1996: The NCEP/NCAR Reanalysis 40-year Project. *Bull. Amer. Meteor. Soc.*, 77, 437–471

Kruse, L., B. Sierk, T. Springer, and M. Cocard, 1999: GPSMeteorology: Impact of Predicted Orbits on Precipitable Water Estimates**,** *Geophys. Res. Let.*, 24, 14, 2045–2048.

Lanzante, J.R., 1996: Resistant, Robust and Non-Parametric Techniques for the Analysis of Climate Data: Theory and Examples, including Applications to Historical Radiosonde Station Data, *Int. J. Climatol.*, 16, 1197–1226.

Lilliefors, H., 1967: On the Kolmogorov-Smirnov test for normality with mean and variance unknown, *J. Am. Statistical Assoc.*, 62, 399–402.

Marcus, S. 2007: Influence of GPS precipitable water vapor retrievals on quantitative precipitation forecasting in southern California, *J. Appl. Meteorology and Climatology*, 46, 1828–1839, DOI: 10.1175/2007JAMC1502.1.

Morland, J., M. Collaud Coen, K. Hocke, P. Jeannet, and C. Mätzler, 2009: Tropospheric water vapour above Switzerland over the last 12 years, *Atmos. Chem. Phys.*, 9, 5975–5988.

Nilsson, T., and G. Elgered, 2008: Long-term trends in the atmospheric water vapor content estimated from ground-based GPS data, *J. Geophys. Res.*, 113, D19101, DOI:10.1029/2008JD010110.

Ohtani, R., and I. Naito, 2000: Comparisons of GPS-derived precipitable water vapors with radiosonde observations in Japan, *J. Geophys. Res.*, 105(D22), 26,917–26,929.

Ortiz de Galisteo, J.P., C. Toledano, V. Cachorro, and B. Torres, 2010: Improvement in PWV estimation from GPS due to the absolute calibration of antenna phase center variation, *GPS Solut.*, 14, 389–395, 2010. DOI 10.1007/s10291-010-0163-y.

Ortiz de Galisteo, J.P., V. Cachorro, C. Toledano, B. Torres, N. Laulainen, Y. Bennouna, and A. de Frutos, 2011: Diurnal cycle of precipitable water vapor over Spain. *Q. J. R. Meteorol. Soc.*, 137: 948–958, DOI:10.1002/qj.811

Pettitt, A.N., 1979: A non-parametric approach to the change-point problem, *Appl. Statist.*, 28(2), 126–135.

Randel, D.L., T.H. Vonder Haar, M.A. Ringerud, G.L. Stephens, T.J. Greenwald, and C.L. Combs, 1996: A new global water vapor dataset, *Bull. Am. Meteorol. Soc.*, 77, 6, 1233–1246.

Ray, R.D., and R.M. Ponte, 2003: Barometric tides from ECMWF operational analyses, *Ann. Geophys.*, 21, 1897-1910, 2003. DOI:10.5194/angeo-21-1897–2003.

Reitan, C.H., 1960: Mean monthly values of precipitable water over the United States, 1946-56, *Mon. Wea. Rev., 88, 25–35*.

Saastamoinen, J., 1972: Atmospheric correction for the troposphere and stratosphere in radio ranging of satellites, in The Use of Artificial Satellites for Geodesy, *Geophys. Monogr. Ser.*, 15, ed. S. W. Henriksen, et al., 247–251, AGU, Washington, D.C..

Seco, A., P.J. González, F. Ramírez, R. García, E. Prieto, C. Yagüe, and J. Fernández, 2009: GPS Monitoring of the tropical storm Delta along the Canary Islands track, November 28-29, 2005, *Pure Appl. Geophys*. 166 (2009) 1519–1531, DOI 10.1007/s00024-009-0502-5.

Schneider, M., P.M. Romero, F. Hase, T. Blumenstock, E. Cuevas, and R. Ramos, 2009: Quality assessment of Izaña's upper-air water vapor measurement techniques: FTIR, Cimel, MFRSR, GPS, and Vaisala RS92, *Atmos. Meas. Tech. Discuss.*, 2, 1625–1662.

Sokal R.R., and P.J. Rohlf, 1969: Introduction to Biostatistics. 2nd edition, 363 pp, W.H. Freeman, New York.

Steigenberger, P., V. Tesmer, M. Krügel, D. Thaller, R. Schmid, S. Vey, and M. Rothacher, 2007: Comparisons of homogeneously reprocessed GPS and VLBI long time-series of tropospheric zenith delays and gradients, *J. Geod.*, 81:503–514, DOI 10.1007/s00190-006-0124-y.

Thomas, I.D., M.A. King, P.J. Clarke, and N.T. Penna, 2011: Precipitable water vapor estimates from homogeneously reprocessed GPS data: An intertechnique comparison in Antarctica, *J. Geophys. Res.*, 116, D04107, DOI:10.1029/2010JD013889.

Toledano, C., V.E. Cachorro, A.M. de Frutos, M. Sorribas, N. Prats, and B.A. de la Morena, 2007: Inventory of African desert dust events over the southwestern Iberian Peninsula in 2000–2005 with an AERONET Cimel Sun photometer, *J. Geophys. Res*.,112, D21201.

Toledano, C., V.E. Cachorro, A. Berjón, A.M. de Frutos, M. Sorribas, B. de la Morena, P. Goloub, 2007: Aerosol optical depth and Angstrom exponent climatology at El Arenosillo AERONET site (Huelva, Spain), *Q. J. R. Meteorol. Soc.*, 133 (624).

Toledano, C., V.E. Cachorro, A.M. de Frutos, B. Torres, M. Sorribas, and B. de la Morena, 2009: Air mass classification and analysis of aerosol types at El Arenosillo (Spain). *J. Appl. Met. Climat.*, 48, 5, 962–981.

Torres, B., V.E. Cachorro, C. Toledano, J.P. Ortiz de Galisteo, A. Berjón, A.M. de Frutos, Y. Bennouna and N. Laulainen, 2010: Precipitable water vapor characterization in the gulf of Cadiz region (southwestern Spain) based on sun photometer, GPS and radiosonde data, *J. Geophys. Res*., 115, D18103, doi:10.1029/2009JD012724.

Tralli, D.M., and S.M. Lichten, 1990: Stochastic estimation of tropospheric path delays in global positioning system geodetic measurements, *Bull. Geod.*, 64, 127–159.

Tuller, S.E., 1968: World distribution of mean monthly and annual precipitable water, *Mon. Wea. Rev.*,96, 785–797.

Wang, J., L. Zhang, and A. Dai, 2005: Global estimates of water-vapor-weighted mean temperature of the atmosphere for GPS applications, *J. Geophys. Res.*, 110, D21101, DOI:10.1029/2005JD006215.

Wang, J., L. Zhang, A. Dai, T. Van Hove, and J. Van Baelen, 2007: A near-global, 2-hourly data set of atmospheric precipitable water from ground-based GPS measurements, *J. Geophys. Res.*, 112, D11107, DOI:10.1029/2006JD007529.

Zveryaev, I.I., J. Wibig, and R.P. Allan, 2008: Contrasting interannual variability of atmospheric moisture over Europe during cold and warm seasons, *Tellus A*, 60:, 32–41. DOI: 10.1111/j.1600-0870.2007.00283.x.

TABLES

Table 1.- Geographical coordinates of the GPS receivers.

GPS sites	Sites acronym	Lat. N	Lon. W	A.S.L. (m)
A Coruña	acor	43º 22’	8º 24’	12
Alicante	alac	38º 20’	0º 29’	10
Almería	alme	36º 51’	2º 28’	77
Cáceres	cace	39º 29’	6º 21’	384
Santander	cant	43º 28’	3º 48’	48
Creus	creu	42º 19’	- 3º 19’	84
Roquetes	ebre	40º 49’	- 0º 30’	58
San Fernando	sfer	36º 28’	6º 12’	40
Valencia	vale	39º 29’	0º 20’	28
Villafranca	vill	40º 27’	3º 57’	596

Table 2.- Statistics of the PWV monthly data series: mean, standard deviation (SD), median, 5^{th} and 95^{th} percentiles, maximum, minimum, coefficient of asymmetry and kurtosis.

Site	Mean mm	SD mm	Median mm	5th Perc. mm	95th Perc. mm	Max. mm	Min. mm	Coef. Asym.	Kurt.
acor	18.5	4.59	17.8	12.4	25.3	27.0	10.1	0.10	-1.30
alac	19.9	6.41	19.1	12.0	29.7	32.5	9.0	0.21	-1.35
alme	19.0	5.57	18.3	12.0	27.4	32.1	8.1	0.17	-1.21
cace	14.9	3.75	15.3	9.3	20.5	22.0	7.1	-0.01	-1.05
cant	18.7	5.61	18.3	11.5	27.0	30.4	9.2	0.19	-1.30
creu	19.0	6.18	18.7	10.7	28.6	30.1	9.5	0.20	-1.36
ebre	20.0	6.93	19.0	11.2	30.5	33.2	8.9	0.24	-1.35
sfer	18.4	4.15	18.3	12.1	25.2	27.9	8.8	0.08	-0.79
vale	19.9	6.98	18.8	11.4	30.7	33.3	8.5	0.25	-1.35
vill	14.5	4.06	14.3	8.8	20.5	22.2	6.8	0.05	-1.32

Table 3.- Determination coefficient, root mean square of the errors, and mean absolute percentage error of the linear regression of PWV on temperature.

Site	**R^2**	**RMSE** mm	**MAPE** %
acor	0.87	1.64	7.56
alac	0.89	2.11	9.12
alme	0.88	1.95	8.83
cace	0.71	2.03	11.61
cant	0.93	1.50	7.10
creu	0.92	1.75	7.97
ebre	0.92	1.97	8.90
sfer	0.68	2.37	10.4
vale	0.87	2.50	10.9
vill	0.81	1.79	10.6

Table 4.- Average PWV at *sfer* in June, July, and August itemized by the predominant aerosol type of each day at the site of El Arenosillo (close to *sfer*) and relative frequency of the predominant aerosol types.

	PWV (mm)			**Freq.**
	Jun.	**Jul.**	**Aug.**	**%**
Marine	20.44	18.99	21.60	49
Continental	23.18	22.09	23.11	13
Biomass burning	25.20	19.35	26.00	2
Desert dust	25.16	24.49	25.36	27
Mixed	23.87	---	28.14	1
Not classified	25.53	18.92	25.74	8

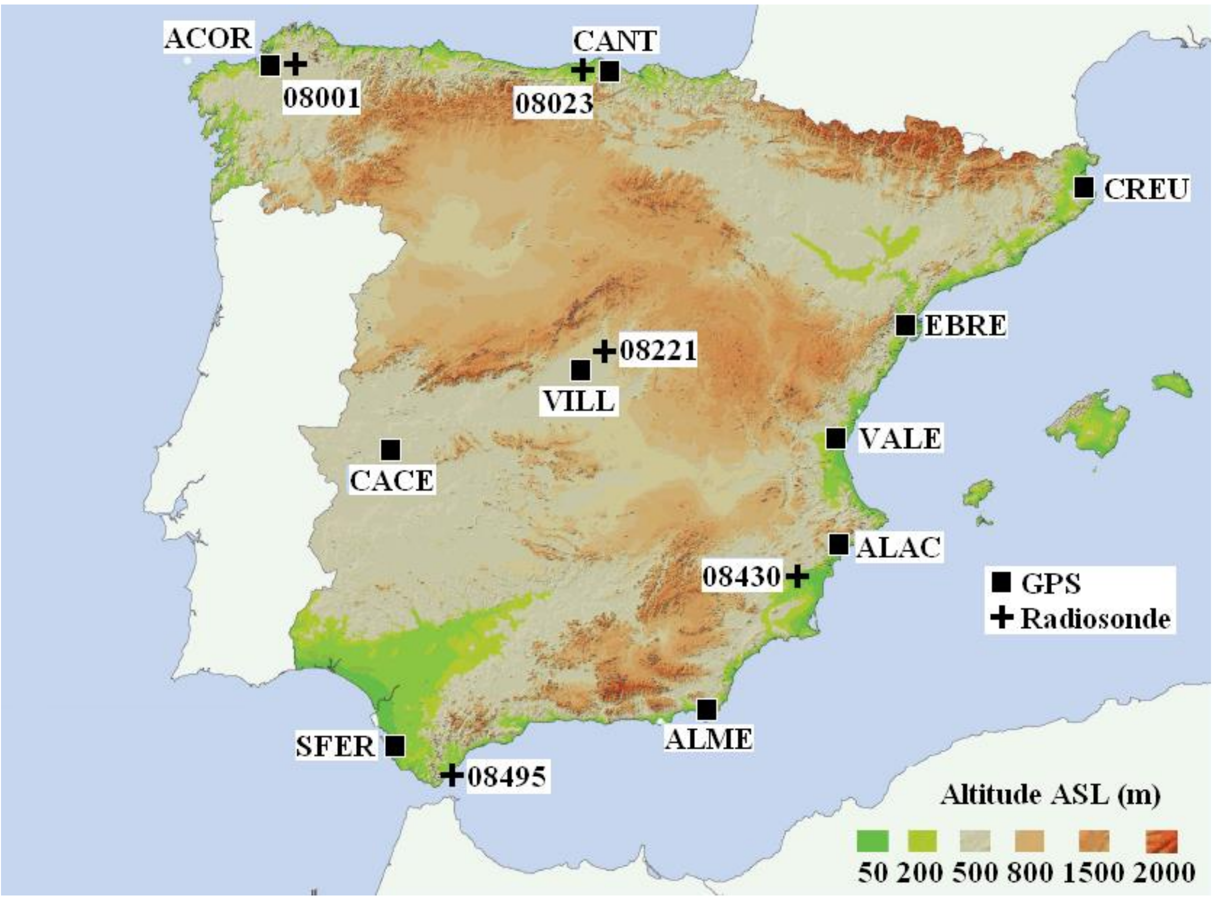

ACOR
08001
CANT
08023
CREU
EBRE
08221
VILL
VALE
CACE
ALAC
08430
GPS
Radiosonde
ALME
SFER
08495
Altitude ASL (m)
50 200 500 800 1500 2000

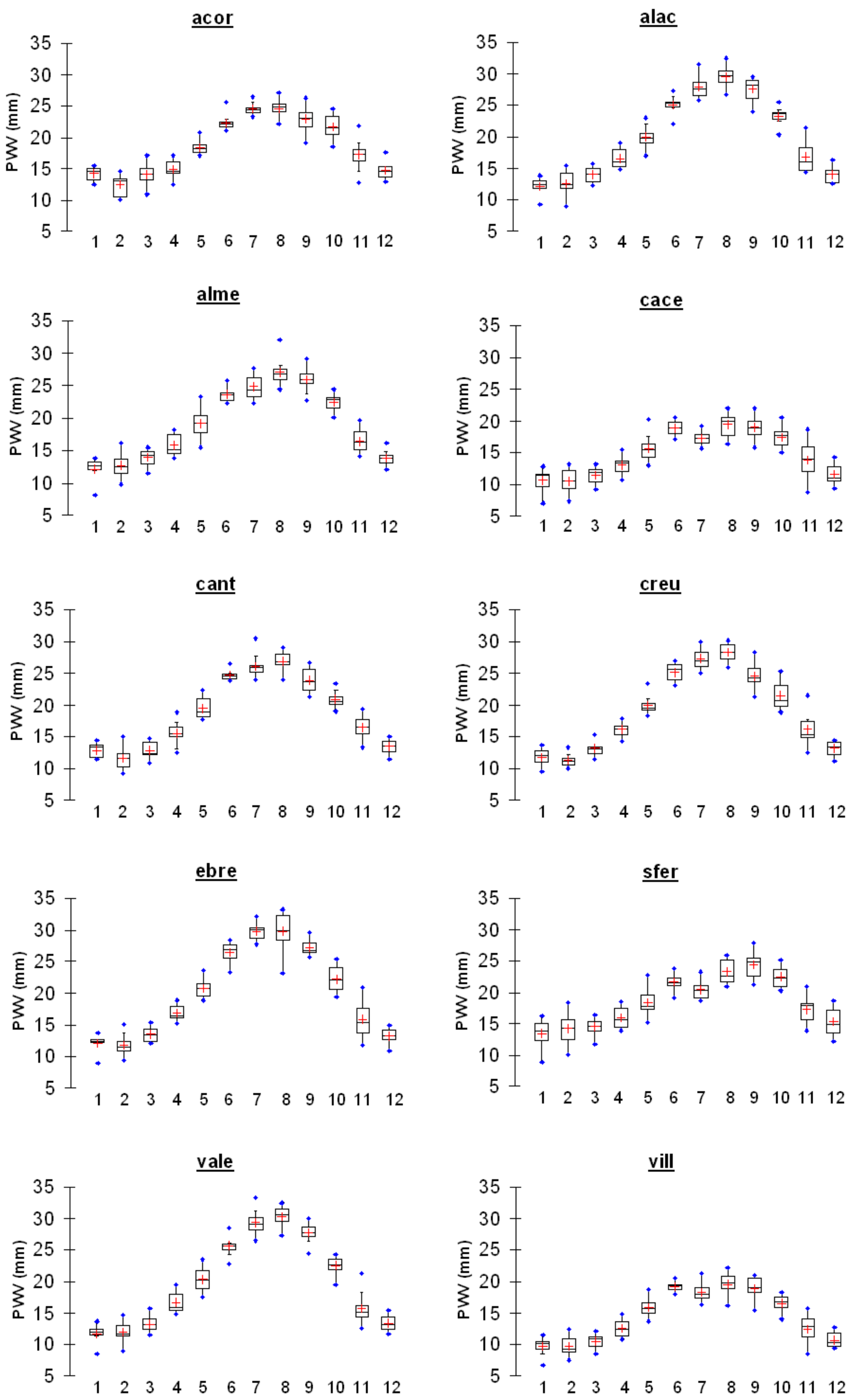
acor
alac
alme
cace
cant
creu
ebre
sfer
vale
vill
PWV (mm)
35
30
25
20
15
10
5
1 2 3 4 5 6 7 8 9 10 11 12

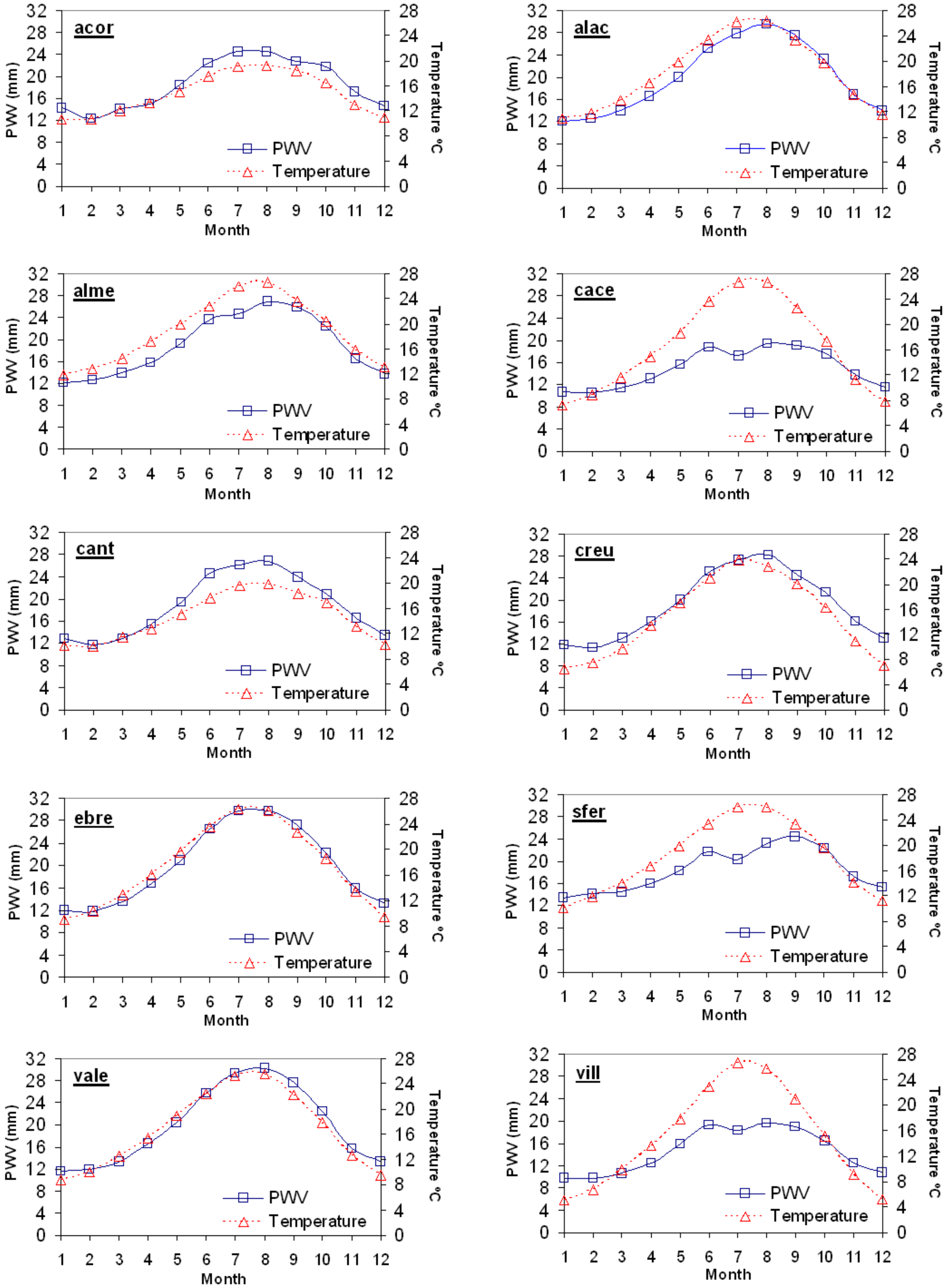
acor
alac
alme
cace
cant
creu
ebre
sfer
vale
vill
PWV (mm)
Temperature °C
Month
PWV
Temperature

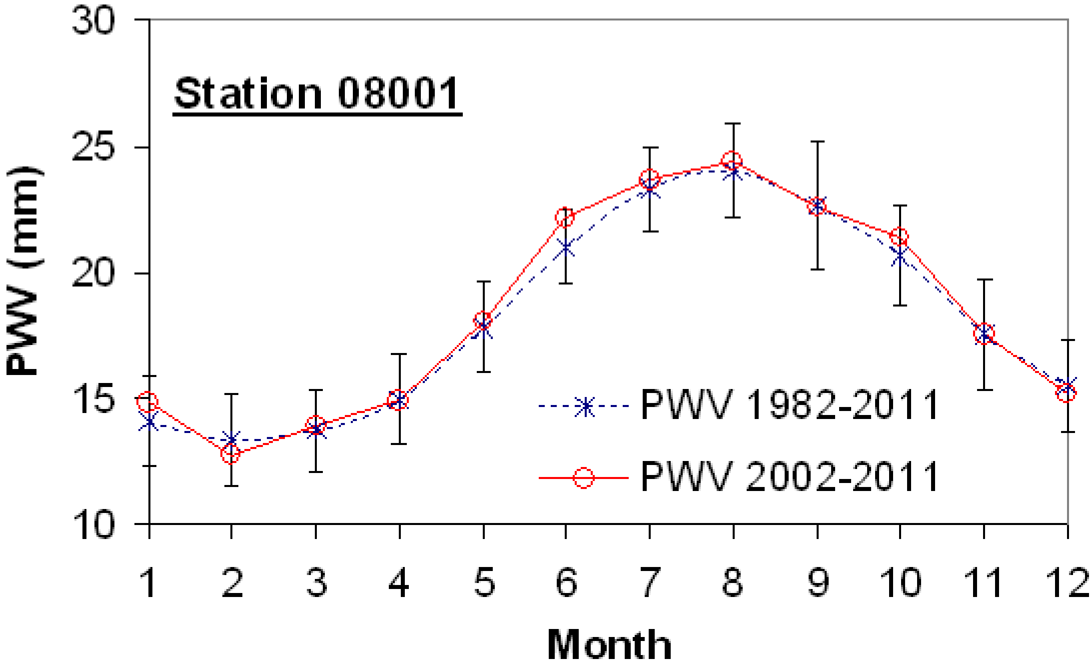
Station 08001
PWV (mm)
30
25
20
15
10
1
2
3
4
5
6
7
8
9
10
11
12
Month
PWV 1982-2011
PWV 2002-2011

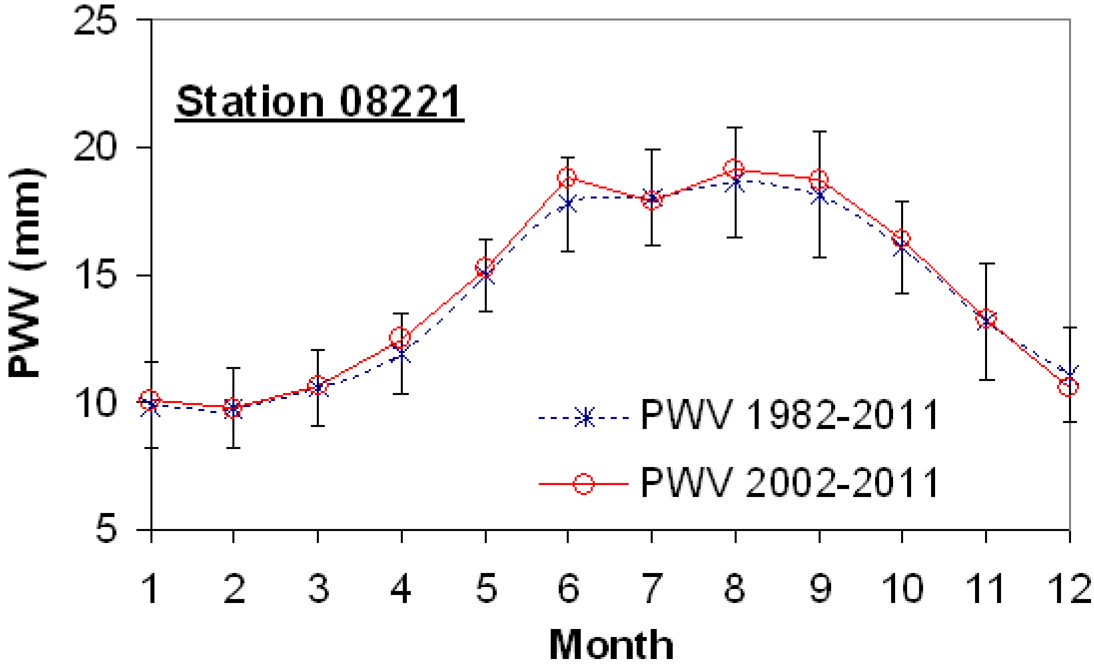
Station 08221
PWV (mm)
25
20
15
10
5
1
2
3
4
5
6
7
8
9
10
11
12
Month
PWV 1982-2011
PWV 2002-2011

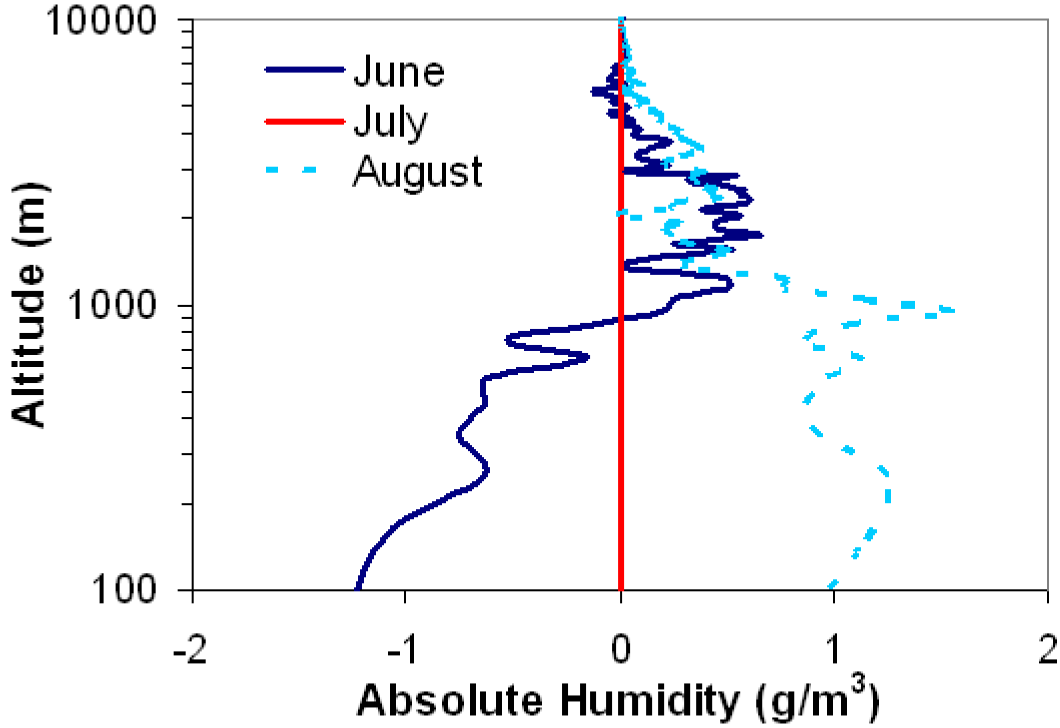

10000
1000
100
Altitude (m)
June
July
August
-2
-1
0
1
2
Absolute Humidity (g/m^3)

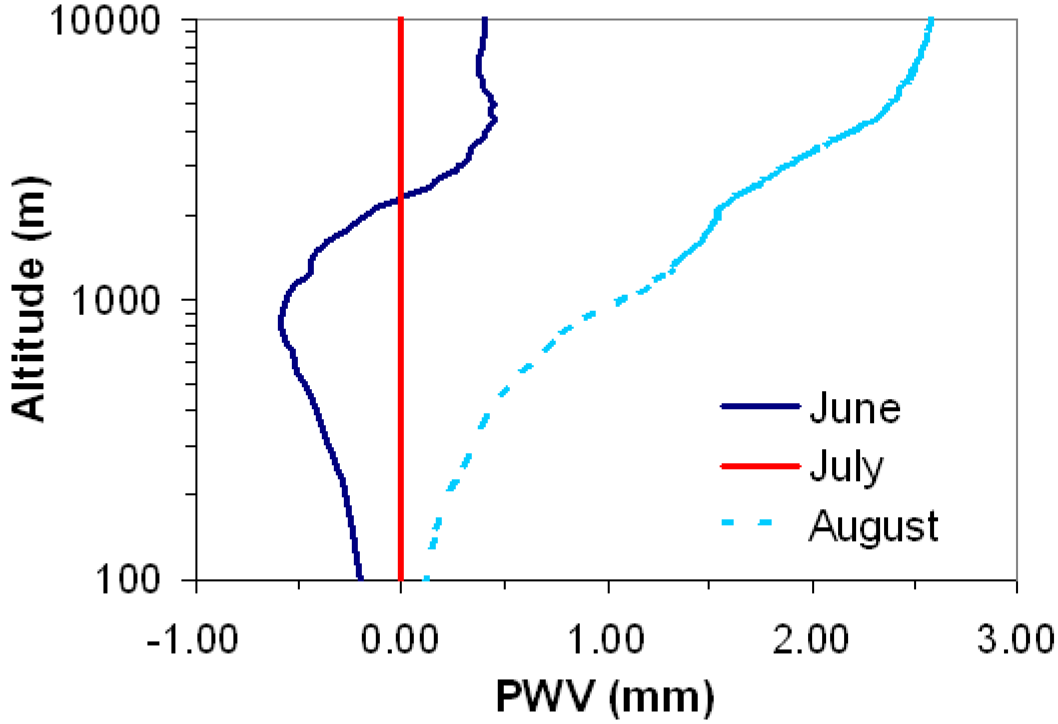

10000
1000
100
Altitude (m)
June
July
August
-1.00
0.00
1.00
2.00
3.00
PWV (mm)

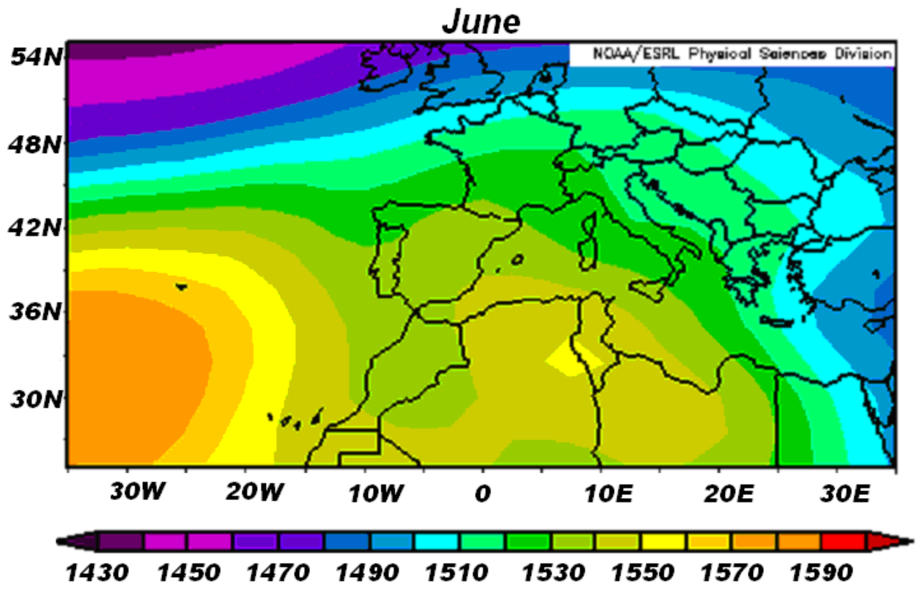
June
NOAA/ESRL Physical Sciences Division
54N
48N
42N
36N
30N
30W
20W
10W
0
10E
20E
30E
1430
1450
1470
1490
1510
1530
1550
1570
1590

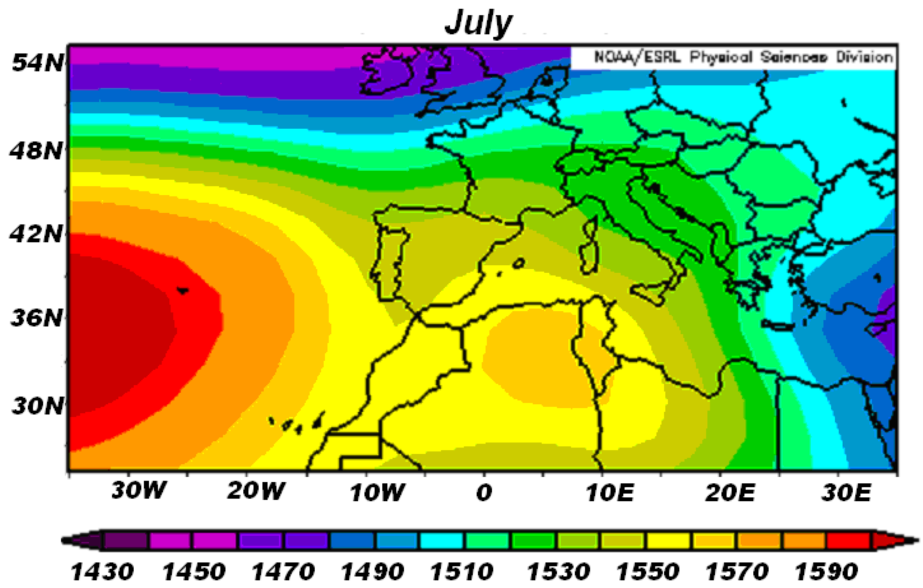
July
NOAA/ESRL Physical Sciences Division
54N
48N
42N
36N
30N
30W
20W
10W
0
10E
20E
30E
1430
1450
1470
1490
1510
1530
1550
1570
1590

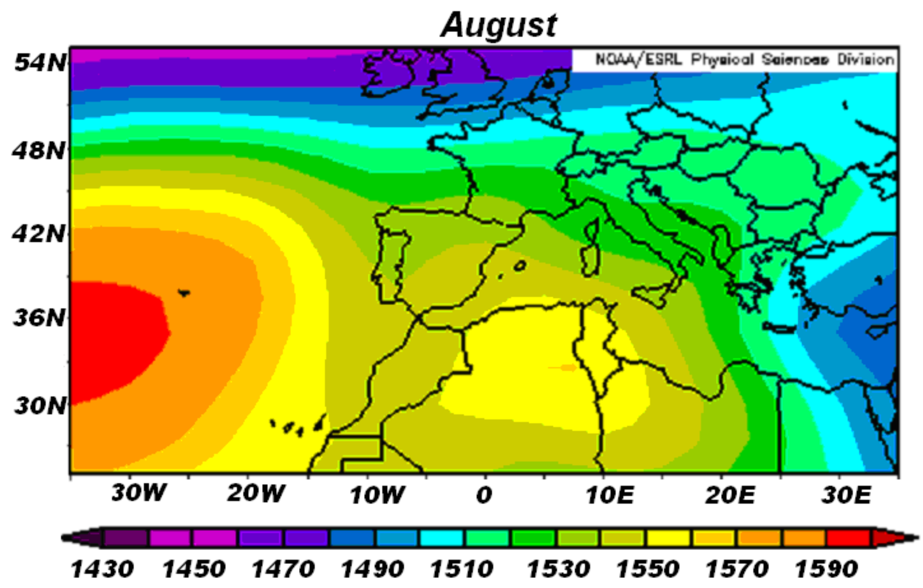
August
NOAA/ESRL Physical Sciences Division
54N
48N
42N
36N
30N
30W
20W
10W
0
10E
20E
30E
1430
1450
1470
1490
1510
1530
1550
1570
1590

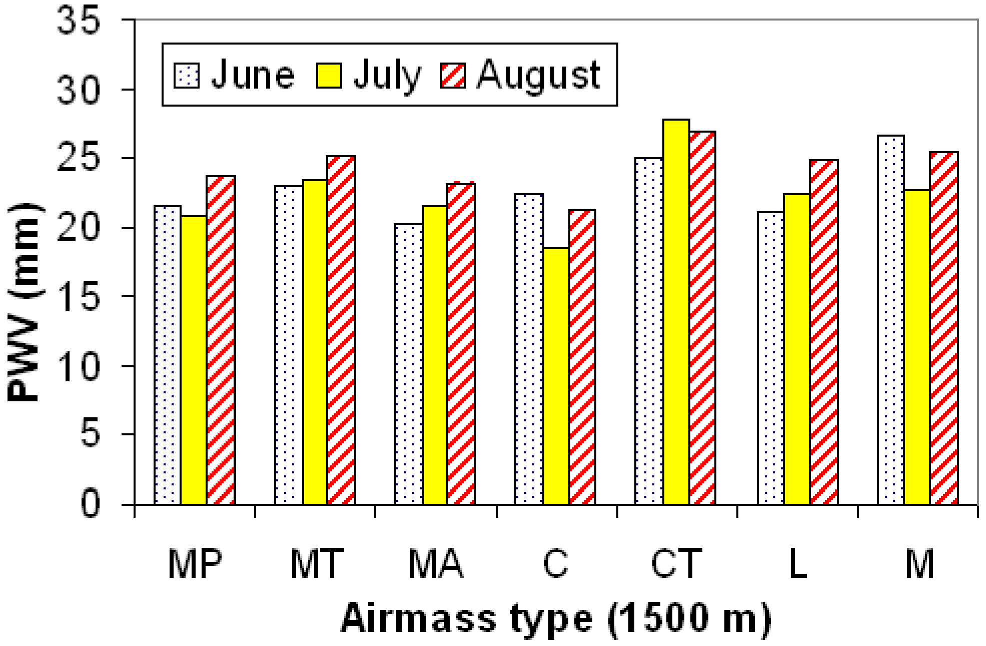

June
July
August
PWV (mm)
0
5
10
15
20
25
30
35
MP
MT
MA
C
CT
L
M
Airmass type (1500 m)